

# VOLTAGE AND FREQUENCY CONTROL OF PARALLEL OPERATED SELF EXCITED INDUCTION GENERATORS

A. H. Al-Bahrani\*

*Electrical Engineering Department  
College of Engineering, King Saud University  
P.O. Box 800, Riyadh 11421, Saudi Arabia*

الخلاصة :

يشرح هذا البحث طريقة تحليلية للتحكم في فرق الجهد والتردد لأي عدد من المولدات الحثية ذاتية الإثارة تعمل على التوازي في ظل ظروف مستقرة ومرتنة . والطريقة المقترحة عامة ويمكن استخدامها لمولد حثي واحد أو لمجموعة من المولدات الحثية المتماثلة أو المختلفة وبسرعات متساوية أو مختلفة . لقد تم التأكد من نتائج الطريقة المقترحة عملياً لعدد من الحالات ، ومن ثم تمت دراسة تأثير بعض البارامترات على خواص التحكم في فرق الجهد والتردد لعدد من الحالات باستخدام مولدات حثية متماثلة ومختلفة ، وبسرعات متساوية ومختلفة أيضاً . ولقد لخصت هذه النتائج في هذا البحث .

## ABSTRACT

This paper describes a method of analysis to control both the common bus voltage and the frequency of any number of parallel operated self-excited induction generators, SEIG's, under steady state balanced conditions. The proposed method is general and can be used for a single or a group of SEIG's employing similar or different machines with equal or unequal speeds. Theoretical predictions of the proposed model have been verified experimentally for a number of configurations. Using this method, effects of various parameters on the voltage and frequency control characteristics are examined for a number of cases employing similar and different SEIG's at equal and unequal speeds and the results are summarized in the paper.

\*Address for correspondence:  
Tig - Tesco International Ltd.  
P.O. Box 647, Dammam 31421  
Saudi Arabia

## VOLTAGE AND FREQUENCY CONTROL OF PARALLEL OPERATED SELF EXCITED INDUCTION GENERATORS

### LIST OF SYMBOLS

$R_{s_i}, R_{r_i}$	= Stator and rotor resistances.
$X_{s_i}, X_{r_i}, X_{m_i}$	= Stator, rotor and magnetizing reactances.
$C, X_c$	= Excitation capacitance and its reactance.
$R_L, X_L, Z_L$	= Load resistance, reactance and impedance.
$G_L, B_L, Y_L$	= Load conductance, susceptance and admittance.
$I_{s_i}, I_{r_i}, I_{m_i}$	= Stator, rotor and magnetizing currents.
$V_{g_i}, v_i$	= Air gap voltage and per unit speed.
$I_L, I_c$	= Load and excitation capacitor currents.
$V_t, f, n$	= Bus voltage, frequency and number of machines.
WRM, SCM	= Wound Rotor Machine and Squirrel Cage Machine.

All quantities are in per unit values; rotor quantities are referred to stator; all reactances are at base frequency; subscript "i" denotes  $i^{th}$  machine; and base capacitance is  $34.97 \mu\text{F}$ .

### 1. INTRODUCTION

Owing to increased emphasis on renewable energy sources due to increasing costs and rapid depletion of conventional energy sources, the development of suitable power generators driven by wind, small hydro-electric, biogas, *etc.* systems has recently assumed greater significance. The capacitor self excited induction generator, SEIG, has emerged as a suitable candidate for such energy sources because of its many advantages [1-6].

In mini hydro and wind generating systems, several SEIG's may have to be operated in parallel in order to exploit the full potential of the energy field. Therefore, studying the performance characteristics of SEIG's in both stand alone and parallel modes is of practical interest [6 and 7].

SEIG's are usually characterized by their poor terminal voltage and frequency regulation under varying load conditions even for fixed prime mover speeds [7-12]. For a single SEIG operating at a constant speed [8] and for parallel operated SEIG's [7], it has been shown that the terminal voltage can be kept constant by increasing the value of the excitation capacitance as the generator load power is increased. However, in this case the frequency drops almost linearly with increasing load power. Alternatively, for a fixed value of the excitation capacitance, the terminal voltage can be kept constant by increasing the prime mover speed as the load power is increased [8]. However, in this case the frequency increases with output power. Thus, if either the excitation capacitance or the prime mover speed is used to control the terminal voltage, the system frequency varies with operating conditions.

This paper shows that it is possible to control both the terminal voltage and frequency simultaneously by adjusting the values of the excitation capacitance and speed of all or some machines which are used in the control process. The proposed method of analysis is general and can be used to show how to maintain constant terminal voltage and frequency in any number of parallel SEIG's under steady state, balanced, varying load conditions. Using this method, the effects of various parameters on the terminal voltage and frequency control characteristics are examined for a number of SEIG configurations in which similar or different machines are operated at equal

or unequal speeds. Detailed results of these investigations are reported along with experimental verification of the proposed model.

## 2. PROPOSED MODEL

Figure 1 shows  $n$  induction machines connected to the same bus across  $C$  and  $Z_L$ . These machines are driven at per unit speeds  $v_1, v_2, \dots, v_n$  respectively. In such a system, all machines will operate at the same terminal voltage and frequency. Figures 2a and b show the per-phase steady state equivalent circuits of the excitation capacitor and load and the  $i^{th}$  machine respectively. To represent the parallel operation of these machines,  $n$  such equivalent circuits (Figure 2b) have to be connected across the circuit of Figure 2a. Consequently, the magnitude of the terminal voltage divided by the per unit frequency can be related to the magnitudes of the total terminal impedance and stator current of each machine by:

$$|Z_i||I_{s_i}| = |V_t|/f \tag{1}$$

for  $i = 1, 2, \dots, n$ . It is important to note that (1) is valid for both actual as well as per unit quantities as long as  $f$  is in per unit. Furthermore, the stator current magnitude,  $|I_{s_i}|$ , can be obtained from the air-gap voltage and the equivalent impedance of the parallel combination of the magnetizing reactance and the rotor circuit, *i.e.*

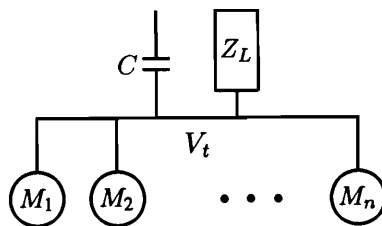


Figure 1. Multi-Induction Machine System.

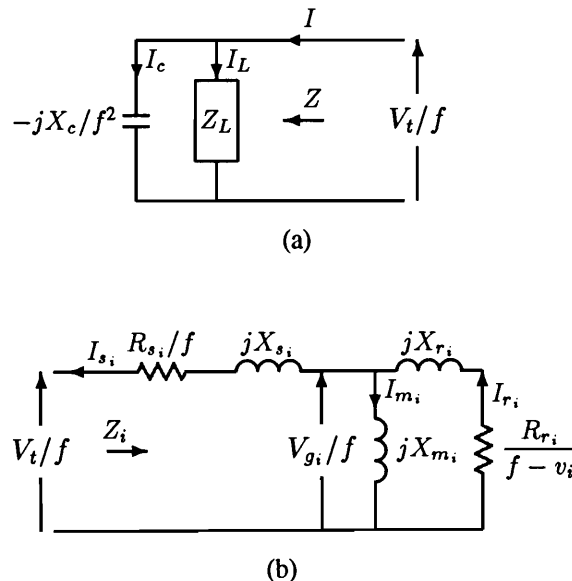


Figure 2. Per Phase Equivalent Circuits of: (a) the Excitation Capacitor and Load, (b) the  $i^{th}$  Induction Machine.

$$|I_{s,i}| = \frac{(|V_{g_i}|/f)}{|Z_{mr,i}|} \quad (2)$$

The magnitude of the air-gap voltage and the magnetizing reactance of each machine can be related by a relationship of the form  $|V_{g_i}|/f = a_i + b_i X_{m_i}$ . Such a relationship can be established experimentally as discussed in [8]. Consequently, (2) becomes

$$|I_{s,i}| = \frac{a_i + b_i X_{m_i}}{|Z_{mr,i}|} \quad (3)$$

Substituting for  $|I_{s,i}|$  from the above equation and rearranging, (1) can be rewritten as:

$$g_i = f|Z_i|(a_i + b_i X_{m_i}) - |V_t||Z_{mr,i}| = 0 \quad (4)$$

for  $i = 1, 2, \dots, n$ . Expressions for  $Z_i$  and  $Z_{mr,i}$  are given in Appendix A.

Under self-excitation, the net current injection at the common bus is zero whereas its voltage is not zero. Therefore, the real and imaginary parts of the total bus admittance must be independently equal to zero, *i.e.*

$$g_{n+1} = G_L + \sum_{i=1}^n G_i = 0 \quad (5)$$

and

$$g_{n+2} = \frac{f^2}{X_c} + B_L + \sum_{i=1}^n B_i = 0 \quad (6)$$

where  $G_L$  and  $B_L$  are the real and imaginary parts of ( $Y_L = 1/Z_L$ ) and  $G_i$  and  $B_i$  are those of ( $Y_i = 1/Z_i$ ). Their corresponding expressions are given in Appendix A. Equations 4 to 6 are  $(n+2)$  nonlinear equations which can be solved for the  $(n+2)$  unknowns. If  $V_t$  and  $f$  are to be kept at specified levels,  $(n+1)$  of the unknowns are  $X_{m_1}, \dots, X_{m_n}$  and  $C$ . The last unknown is  $v$  which is the speed of the SEIG's used in the control process. The controlling machines are assumed to have a common variable speed,  $v$ , while the remaining machines may have fixed speeds. Along with  $C$ ,  $v$  may be used to control both  $V_t$  and  $f$ .

Assume that the first " $j$ " ( $1 \leq j \leq n$ ) of the " $n$ " parallel SEIG's are the controlling machines and the remaining  $(n-j)$  SEIG's have fixed speeds. For known values of  $v_{j+1}, v_{j+2}, \dots, v_n, Z_L, V_t, f$  and machines parameters, (4) to (6) can be solved for  $X_{m_1}, \dots, X_{m_n}, C$  and  $v$  using the Newton Raphson method. Upon linearization, (4) to 6 can be expressed in the following partitioned form:

$$\begin{pmatrix} g_x \\ g_y \end{pmatrix} = - \begin{pmatrix} K & L \\ M & N \end{pmatrix} \begin{pmatrix} \Delta x \\ \Delta y \end{pmatrix} \quad (7)$$

where

$$g_x = (g_1 \quad g_2 \quad \dots \quad g_n)^t \quad (8)$$

$$g_y = (g_{n+1} \quad g_{n+2})^t, \quad (9)$$

$$\Delta x = ( \Delta X_{m_1} \quad \Delta X_{m_2} \quad \cdots \quad \Delta X_{m_n} )^t \quad (10)$$

$$\Delta y = ( \Delta C \quad \Delta v )^t \quad (11)$$

Submatrices  $K$ ,  $L$ ,  $M$ , and  $N$  of the Jacobian are defined as follows.  $K$  is a diagonal matrix with elements

$$k_{ii} = \frac{\partial g_i}{\partial X_{m_i}}, \quad i = 1, 2, \dots, n \quad (12)$$

$$L = \begin{pmatrix} 0 & 0 & 0 & 0 & \cdots & 0 \\ \frac{\partial g_1}{\partial v} & \cdots & \frac{\partial g_j}{\partial v} & 0 & \cdots & 0 \end{pmatrix}^t \quad (13)$$

$$M = \begin{pmatrix} \frac{\partial g_{n+1}}{\partial X_{m_1}} & \frac{\partial g_{n+1}}{\partial X_{m_2}} & \cdots & \frac{\partial g_{n+1}}{\partial X_{m_n}} \\ \frac{\partial g_{n+2}}{\partial X_{m_1}} & \frac{\partial g_{n+2}}{\partial X_{m_2}} & \cdots & \frac{\partial g_{n+2}}{\partial X_{m_n}} \end{pmatrix} \quad (14)$$

$$N = \begin{pmatrix} 0 & \frac{\partial g_{n+1}}{\partial v} \\ \frac{\partial g_{n+2}}{\partial C} & \frac{\partial g_{n+2}}{\partial v} \end{pmatrix} \quad (15)$$

where

$$\frac{\partial g_{n+1}}{\partial v} = \sum_{i=1}^j \frac{\partial G_i}{\partial v} \quad (16)$$

and

$$\frac{\partial g_{n+2}}{\partial v} = \sum_{i=1}^j \frac{\partial B_i}{\partial v} \quad (17)$$

Since  $K$  is a diagonal matrix,  $K^{-1}$  can be found directly. Subsequently,  $\Delta y$  and  $\Delta x$  can be evaluated as follows:

$$\Delta y = -(N - MK^{-1}L)^{-1}(g_y - MK^{-1}g_x) \quad (18)$$

$$\Delta x = -K^{-1}(g_x + L\Delta y) \quad (19)$$

It is clear that finding  $\Delta y$  involves the solution of only two equations. Once  $\Delta y$  is found,  $\Delta x$  can be calculated easily from (19). Consequently, the values of the unknown variables can be updated for the next iteration. This process is continued until convergence to the correct solution is obtained.

### 3. RESULTS AND DISCUSSION

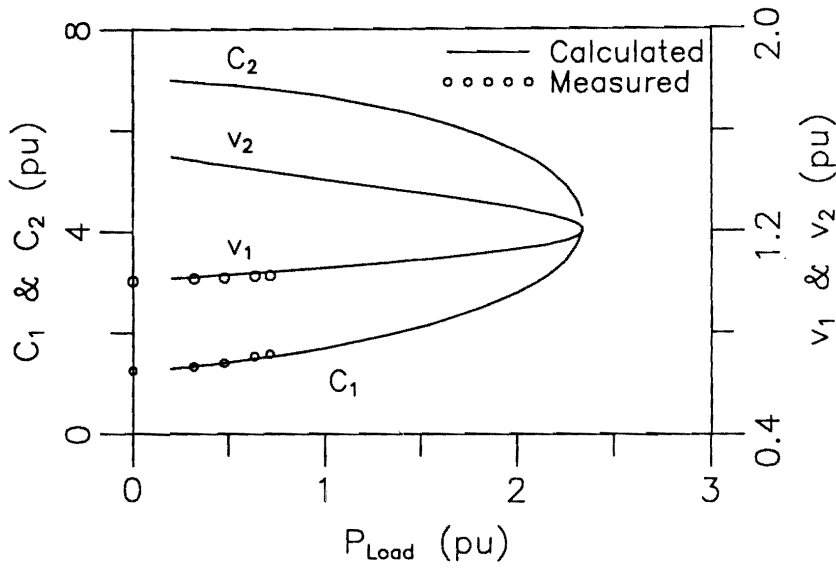
In order to test the validity of the proposed model and to investigate the voltage control and frequency characteristics of parallel operated SEIG's, two types of machines are used; namely, a squirrel cage machine (SCM) and a wound rotor machine (WRM). Data for these machines are given in Appendix B. It is important to note that the differences in characteristics which are shown in Figures 3b, 3c, 4b, 5b, 6b, 7b, 9, and 10 are caused by the difference in the machine parameters and not by the difference in the machine type. Machine type (WRM & SCM) is used only to identify the machines that are under study.

It is found that, for voltage and frequency control there are two possible solutions of  $C$  and  $v$  depending upon the initial conditions used in the numerical iterative computations. If the unsaturated magnetizing reactance of each machine is used as the initial value for the corresponding machine magnetizing reactance,  $X_{m_i}$ ,  $1.05f$  as the initial value of  $v$ , and the initial value of  $C$  is selected such that  $X_c = -f^2/(B_L + \sum_{i=1}^n B_i)$ , the solution converges to  $C_1$  and  $v_1$  (lower  $C$  and  $v$  values) which will be referred to as the first solution. However, if the initial value of  $v$  is taken as  $1.5f$  and the initial value of  $C$  is selected such that  $X_c = -f^2/4(B_L + \sum_{i=1}^n B_i)$ , the solution converges to  $C_2$  and  $v_2$  (higher  $C$  and  $v$  values) which will be referred to as the second solution. Once  $C$  and  $v$  are known,  $X_{m_1}, \dots, X_{m_n}$  can be easily calculated from Equation 19. Consequently, the complete performance characteristics of all machines can be easily evaluated using the appropriate equations given in Appendix C.

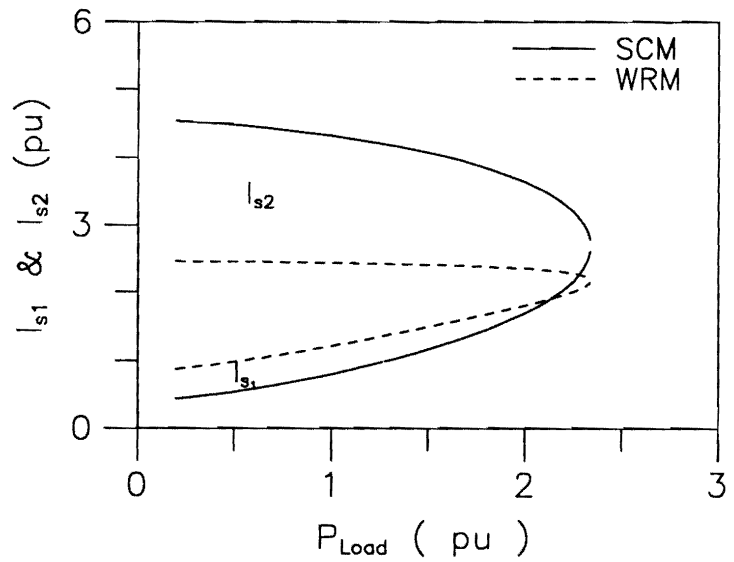
Figure 3a shows calculated and measured variations of  $C$  and  $v$  with  $P_{Load}$  when the WRM and the SCM, which were operated in parallel, had the same shaft speed,  $v$ , and were feeding a balanced resistive load. By varying  $C$  and  $v$ ,  $V_i$  as well as  $f$  were kept constant at 1 pu. There are two solutions ( $C_1, v_1$  and  $C_2, v_2$ ) as mentioned earlier. It is interesting to note that at a certain maximum power,  $(P_{Load})_{max}$ , the two solutions merge.  $(P_{Load})_{max}$  represents the maximum theoretical power which the system can supply under the specified conditions. It is obvious that the actual output power of the system will be lower than  $(P_{Load})_{max}$  and will be dictated by the ohmic losses and associated heating of the windings.

Figures 3b and c show the variations of stator currents and efficiencies of the two machines with  $P_{Load}$  for the same operating conditions mentioned above. Here  $I_{s1}, I_{s2}, \eta_1$ , and  $\eta_2$  refer to stator currents and efficiencies corresponding to the first and the second solutions respectively. It is clear that corresponding to the second solution, the currents are unacceptably high and the machines have very low values of efficiency over the range of practical interest. Thus, for practical use, only the first solution is recommended since it requires lower values of  $C$  and  $v$ , has lower values of stator currents and exhibits higher efficiencies. It is clear from Figure 3 that the calculated and measured variations of  $C_1$  and  $v_1$  with  $P_{Load}$  are in good agreement verifying the validity of the proposed model. No attempt was made to verify the second solution due to the very large  $C$  values required and the unacceptably high values of currents associated with this solution.

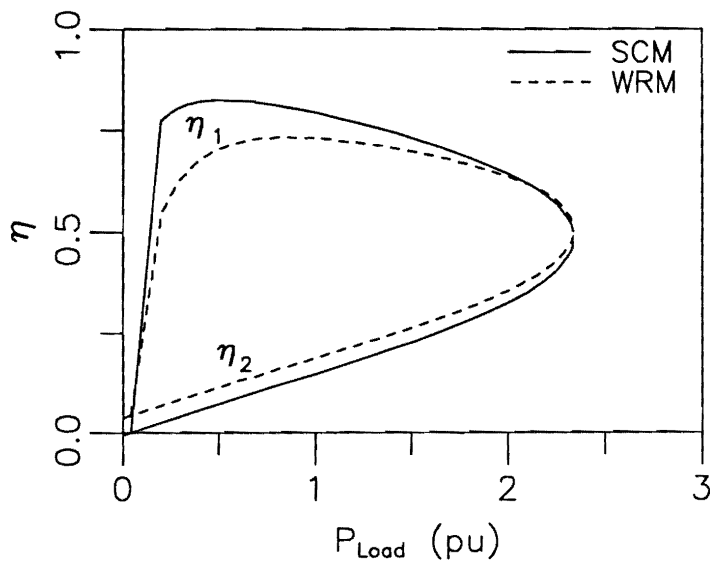
In a multi-machine system, it is possible to keep the speeds of some of the machines at fixed values and control the bus frequency by changing the speed of the rest of the machines. Figure 4a shows the calculated and measured variations of  $v$  and  $C$  to keep  $V_i$  and  $f$  at 1 pu for a resistive load. For this case, the WRM has



(a). Critical Values of C and v.



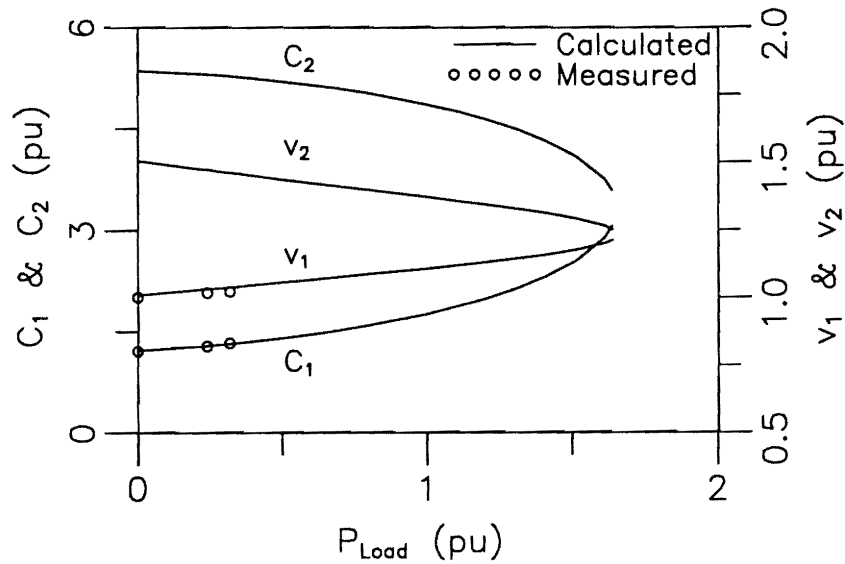
(b).  $I_{s1}$  and  $I_{s2}$ .



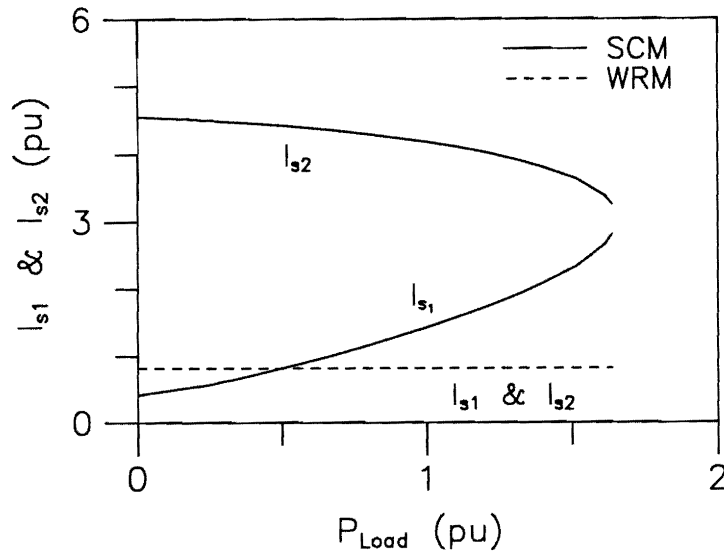
(c). Efficiency,  $\eta$ .

Figure 3. Variation of C, v,  $I_{s1}$ ,  $I_{s2}$ , and  $\eta$  with  $P_{Load}$  when the WRM and the SCM are on the Same Shaft and Feeding a Resistive Load with  $V_t$  and f at 1 pu.

a constant speed of 1 pu and operates in parallel with the SCM whose speed  $v$  is variable. Figure 4b shows the corresponding currents for the two machines. It is clear that, as expected, the WRM has constant values of  $I_s$ , irrespective of the value of  $P_{Load}$ . Moreover, for this machine,  $I_s$  is the same for the two solutions. (i.e.  $I_{s1} = I_{s2}$ ) However, for the SCM,  $I_{s1}$  and  $I_{s2}$  are different and vary with  $P_{Load}$ . Similarly, WRM can be used as the controlling machine. In such a case, SCM has a speed of 1 pu whereas the speed of WRM is  $v$ . For this case, the results are shown in Figure 5. As expected, the speed,  $v_1$ , as well as stator current,  $I_{s1}$  of the WRM increase with  $P_{Load}$  whereas for the SCM,  $I_{s1} = I_{s2} = \text{constant}$ . It is clear from Figures 4 and 5 that with the SCM, frequency control is possible over a wider range of  $P_{Load}$  values as compared to the case when the WRM is used for control purposes. This is due to the different parameters and magnetization characteristics of the two machines. Figures 4 and 5 show a good agreement between the measured and calculated values of  $v_1$  and  $C_1$ .



(a) Critical Values of C and v.

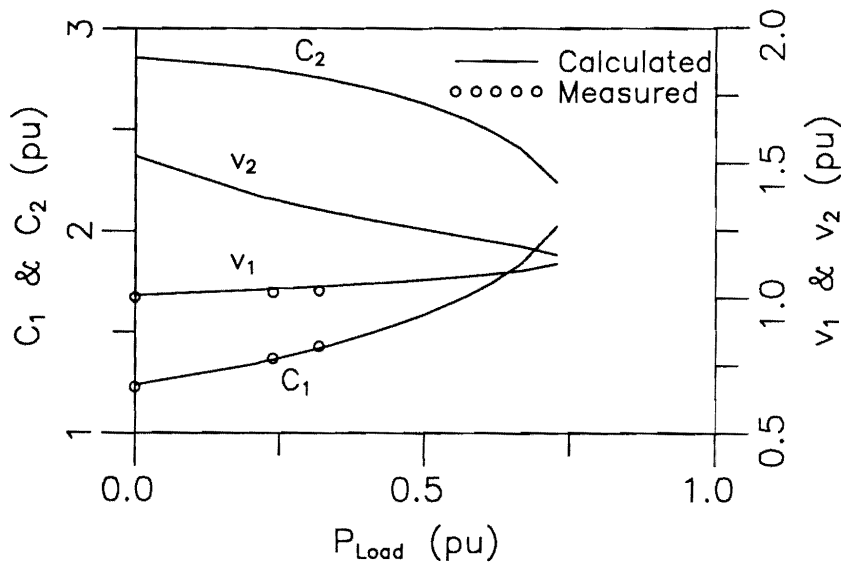


(b)  $I_{s1}$  and  $I_{s2}$ .

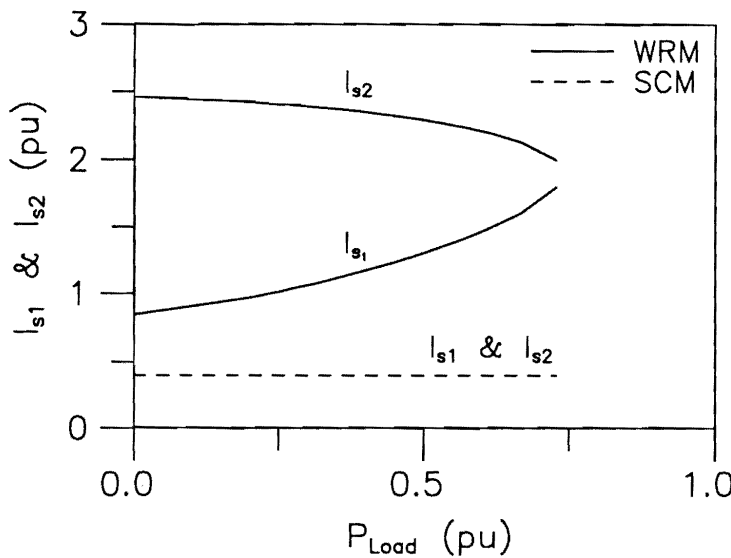
Figure 4. Effect of  $P_{Load}$  on C, Speed of the SCM, v, and  $I_s$  when the Speed of WRM,  $V_t$ , and f are all at 1 pu.

It is clear from the discussion so far that the values of  $C$  and  $v$  required to hold  $V_t$  and  $f$  constant depend upon  $P_{Load}$  and the parameters and characteristics of all machines. In addition, the  $C$  and  $v$  values also depend upon the desired value of  $V_t$ ,  $f$ , load power factor and characteristics of the machines. Figure 6a shows variations of  $C$  and  $v$  for different values of  $V_t$  when the WRM and the SCM have the same speed,  $v$ , with  $f = 1$  pu and feeding a resistive load. In this and the subsequent figures, only the first solution is shown.

It is clear from Figure 6a that for a given value of  $P_{Load}$ , both  $C$  and  $v$  vary with  $V_t$  in a nonlinear fashion. Similarly the machines currents also vary in a nonlinear fashion with  $P_{Load}$  and  $V_t$ . Under these conditions, the variations of currents are different for the two machines as shown in Figure 6b. Similarly the efficiency of each machine depends on both  $P_{Load}$  and  $V_t$ .



(a) Critical Values of  $C$  and  $v$ .



(b)  $I_{s1}$  and  $I_{s2}$ .

Figure 5. Effect of  $P_{Load}$  on  $C$ , Speed of the WRM,  $v$ , and  $I_s$  when the Speed of SCM,  $f$ , and  $V_t$  are all at 1 pu.

Figure 7a shows variations of  $C$  and  $v$  with  $P_{Load}$  for different values of  $f$  when the WRM and the SCM are on the same shaft and feeding a resistive load with  $V_t = 1$  pu. Figure 7b shows the corresponding variations of the currents for both machines. It is clear from this figure that, for a given value of  $P_{Load}$ , when  $f$  is increased  $C$  decreases and  $v$  increases. Moreover,  $I_s$  decreases for both machines as  $f$  is increased. Consequently, the system efficiency is also influenced by the value of  $f$ .

The effect of load power factor,  $pf$ , on the capacitance requirements when the WRM and the SCM are operated in parallel and have the same speed as illustrated in Figure 8. For this case,  $V_t$  and  $f$  are kept at 1 pu. As expected, the capacitance requirements are influenced by load power as well as its power factor. However, for a given value of load power, the load power factor does not influence  $v$ . Consequently, the variation between  $v$  and  $P_{Load}$  for any value of load power factor will be as shown earlier in the  $v_1-P_{Load}$  curve of Figure 3a.

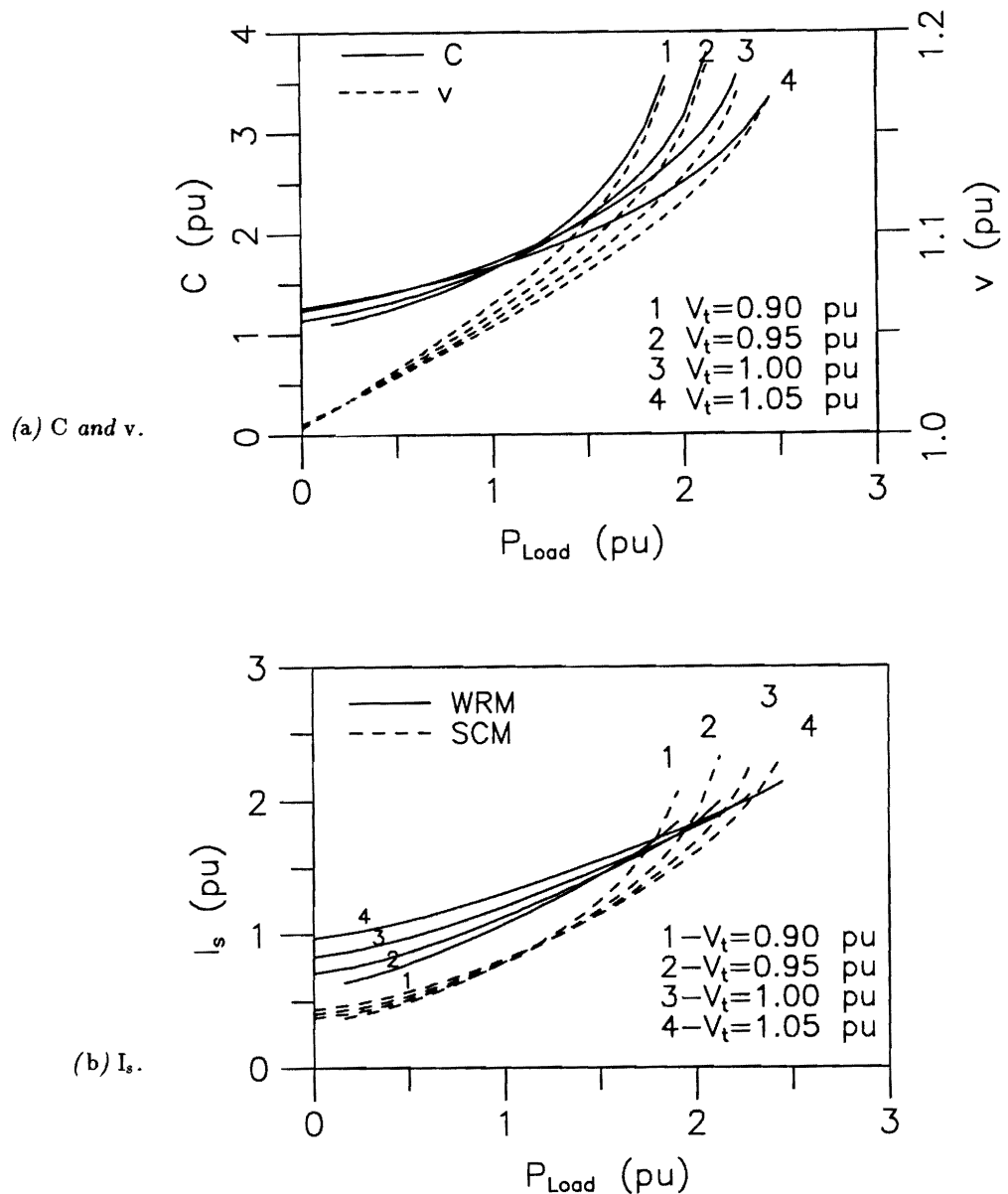
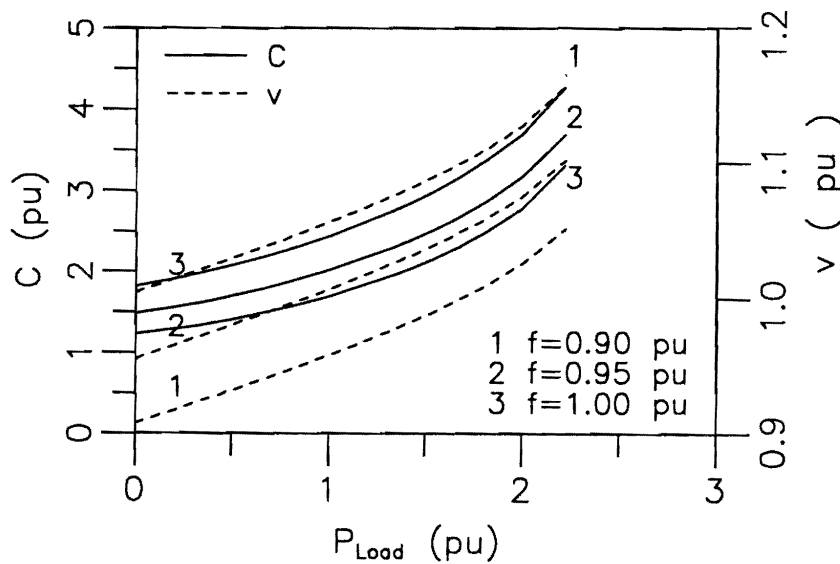


Figure 6. Effect of  $V_t$  and  $P_{Load}$  on  $C$ ,  $v$ , and  $I_s$  when the WRM and SCM were on the Same Shaft with  $f = 1$ .

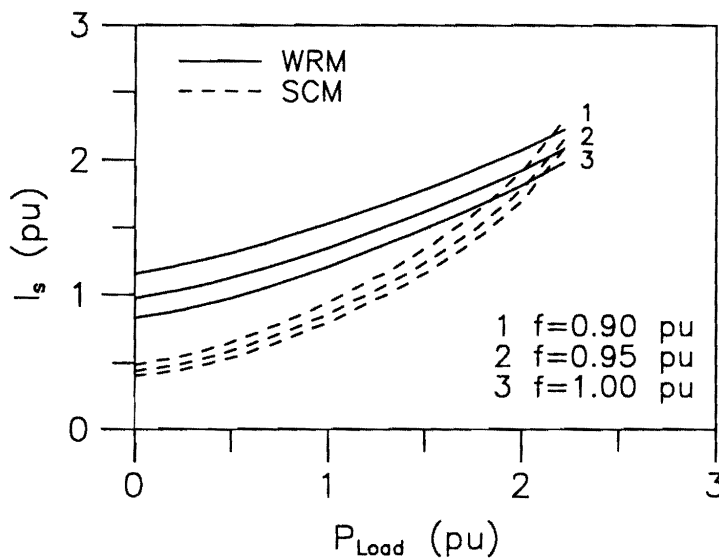
Moreover, for a given value of  $P_{Load}$ , the stator currents and machine efficiencies are not influenced by the load power factor. Hence, machine speeds, currents and efficiencies will remain unchanged with variation of load power factor for given values of  $P_{Load}$ ,  $V_t$  and  $f$ . However, the values of  $C$  required to keep  $V_t$  and  $f$  constant will depend upon load power factor as discussed above.

If  $C$  and only one machine speed are used to control  $V_t$  and  $f$ , the influence of load power factor is similar to that discussed above. However, in this case, somewhat higher capacitance is required.

Figure 9 shows the effect of the number of machines, having the same speed  $v$ , on the  $C$ - $P_{Load}$  and  $v$ - $P_{Load}$  variations with  $V_t$  and  $f$  at 1 pu for a resistive load. It is clear from this figure that the values of  $C$  and  $v$



(a)  $C$  and  $v$ .



(b)  $I_s$ .

Figure 7. Effect of  $f$  and  $P_{Load}$  on  $C$ ,  $v$ , and  $I_s$  when the WRM and SCM were on the Same Shaft with  $V_t = 1$ .

depend upon  $P_{Load}$  as well as the number and characteristics of the machines. Generally, for a given value of  $P_{Load}$ ,  $C$  increases as the number of parallel operated SEIG's is increased. Furthermore, for a given value of  $P_{Load}$ ,  $v$  decreases as the number of parallel SEIG's is increased. This is to be expected since, for a fixed value of  $P_{Load}$ , an increase in the number of parallel connected SEIG's will increase the total rating of the system, thereby decreasing the relative load of each machine.

4. CONCLUSIONS

This paper shows that it is possible to control the terminal voltage and frequency of a single SEIG or a group of SEIG's operating in parallel under steady state balanced operation. The following conclusions can be drawn:

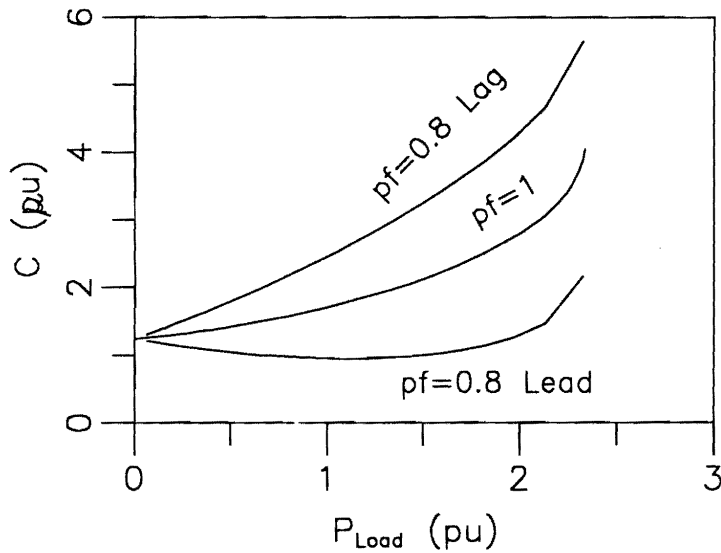


Figure 8. Influence of pf and  $P_{Load}$  on  $C$ .

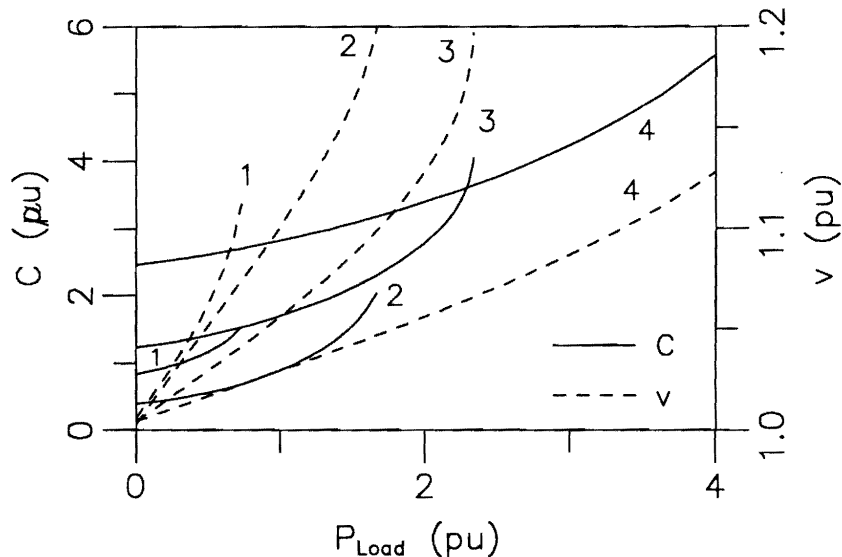


Figure 9. Influence of the Number of Machines and  $P_{Load}$  on  $C$  and  $v$  when the Machines were on the Same Shaft with  $V_t = 1$  pu and  $f = 1$  pu. (1) only one WRM, (2) only one SCM, (3) one WRM and one SCM, (4) two identical WRM's and two identical SCM's.

1. The terminal voltage and frequency of parallel operated SEIG's can be controlled by varying both the excitation capacitance and speed of some or all SEIG's. The value of the capacitance, required to keep both the terminal voltage and frequency constant under a changing load, can be easily calculated by the method shown in this paper. This value depends on the load power, load power factor, terminal voltage as well as the number, parameters, speeds of the controlling SEIG's and magnetizing characteristics of the individual machines. However, for a given load power, the load power factor does not influence  $v$ .
2. The currents and efficiencies of SEIG's vary with load power and terminal voltage in a nonlinear fashion and depend upon the values of the excitation capacitance, speed and parameters of the SEIG's.

## 5. REFERENCES

- [1] D.B. Watson, J. Arrillaga, and T. Densem, "Controllable d.c. Power Supply From Wind-Driven Self-Excited Induction Machines", *Proc. IEE*, **126**(12) (1979), pp. 1245-1248.
- [2] I.P. Milner and D.B. Watson, "An Autonomous Wind Energy Converter Using the Self-Excited Induction Generator for Heating Purposes", *Wind Engineering*, **6**(1) (1982), pp. 19-23.
- [3] Y. Uctug and M. Demirekler, "Modeling, Analysis and Control of a Wind-Turbine Driven Self-Excited Induction Generator", *Proc. IEE*, **135**(4) (1988), pp. 268-275.
- [4] G. Raina and O.P. Malik, "Wind Energy Conversion Using a Self-Excited Induction Generator", *IEEE Trans. on Power App. and Sys.*, **PAS-102**(12) (1983), pp. 3933-3936.
- [5] E.P. Giddens, W. Spittal, and D.B. Watson, "Small-Hydro From a Submersible Pump", *Water and Power Dam Construction*, **34** (1982), pp. 33-35.
- [6] D.B. Watson and I.P. Milner, "Autonomous and Parallel Operation of Self-Excited Induction Generators", *Int. J. Elect. Eng. Education*, **22** (1985), pp. 365-374.
- [7] A.H. Al-Bahrani and N.H. Malik, "Voltage Control of Parallel-Operated Self-Excited Induction Generators", *IEEE, PES Summer Meeting, 1992, Paper # 92 SM 549-6 EC*.
- [8] N.H. Malik and A.H. Al-Bahrani, "Influence of the Terminal Capacitor on the Performance Characteristics of a Self-Excited Induction Generator", *IEE Proc. (C)*, **137**(2) (1990), pp. 168-173.
- [9] A.H. Al-Bahrani and N.H. Malik, "Steady-State Analysis of Parallel-Operated Self-Excited Induction Generators", *Proc. IEE (C)*, **140**(1) (1993), pp. 49-55.
- [10] N.H. Malik and S.E. Haque, "Analysis and Performance of an Isolated Self Excited Induction Generator", *IEEE Trans. on Energy Conversion*, **EC-1**(3) (1986), pp. 134-140.
- [11] A.K. Tandon, S.S. Murthy, and G.J. Berg, "Steady State Analysis of Capacitor Self Excited Induction Generators", *IEEE Trans. on Power App. and Sys.*, **PAS-103**(3) (1984), pp. 612-618.
- [12] S.S. Murthy, O.P. Malik, and A.K. Tandon, "Analysis of Self Excited Induction Generator", *Proc. IEE (C)*, **129**(6) (1982), pp. 260-265.

Paper Received 8 December 1993; Revised 20 March 1994; Accepted 2 April 1994.

## 6. APPENDICES

### A. Derivation of Expressions Used in the Paper

The per phase equivalent circuit of the excitation capacitor and load is shown in Figure 2a. In this Figure (and also in Figure 1), if the load is a series  $R$ - $L$  circuit, then the per phase load impedance is

$$Z_L = R_L/f + jX_L \quad (20)$$

and hence the corresponding load admittance is given by:

$$Y_L = G_L + jB_L = \frac{fR_L}{R_L^2 + f^2X_L^2} - j\frac{f^2X_L}{R^2 + f^2X_L^2} \quad (21)$$

where  $X_L$  is the load inductive reactance at base frequency. On the other hand, if the load is a series  $R$ - $C$  circuit, then

$$Z_L = R_L/f - jX_L/f^2 . \quad (22)$$

Consequently, the corresponding load admittance will be

$$Y_L = G_L + jB_L = \frac{f^3R_L}{f^2R_L^2 + X_L^2} + j\frac{f^2X_L}{f^2R_L^2 + X_L^2} \quad (23)$$

where  $X_L$ , in this case, is the load capacitive reactance at base frequency. From Figure 2b, the equivalent impedance of the parallel magnetizing and rotor circuits for machine "i" is given by:

$$Z_{mr_i} = R_{mr_i} + jX_{mr_i} \quad (24)$$

where

$$R_{mr_i} = \frac{(f - v_i)X_{m_i}^2/R_{r_i}}{1 + (f - v_i)^2(X_{r_i} + X_{m_i})^2/R_{r_i}^2} \quad (25)$$

and

$$X_{mr_i} = X_{m_i} \frac{1 + X_{r_i}(f - v_i)^2(X_{r_i} + X_{m_i})/R_{r_i}^2}{1 + (f - v_i)^2(X_{r_i} + X_{m_i})^2/R_{r_i}^2} . \quad (26)$$

Also the total terminal impedance of machine "i" is given by:

$$Z_i = R_i + jX_i \quad (27)$$

where

$$R_i = R_{s_i}/f + R_{mr_i} \quad (28)$$

and

$$X_i = X_{s_i} + X_{mr_i} . \quad (29)$$

The corresponding machine "i" total admittance is given by:

$$Y_i = G_i + jB_i = \frac{1}{Z_i} = \frac{R_i}{R_i^2 + X_i^2} - j\frac{X_i}{R_i^2 + X_i^2} . \quad (30)$$

**B. Machines Data**

The two test machines are three-phase, 380 V (line), 60 Hz, 4-pole, 1 kW. Base values of frequency, speed and impedance are 60 Hz, 1800 rpm, and 75.86 Ω respectively. The per-unit parameters of the two machines are given in Table 1 below:

**Table 1. Machines Parameters.**

m/c	$R_s$	$R_r$	$X_s = X_r$
SCM	0.16543	0.09324	0.1060
WRM	0.09175	0.06354	0.2112

The measured per-unit variations of the air-gap voltages  $|V_g|/f$ , based on a 220 V, with  $X_m$  for the two machines are shown in Figure 10. These variation are approximated over the practical range of interest as follows: for the SCM,

$$\frac{|V_g|}{f} = \begin{cases} 2.4408 - 0.6080X_m, & X_m \leq 2.384 \\ 3.4592 - 1.0352X_m, & 2.384 \leq X_m \leq 2.812 \\ 9.7841 - 3.2848X_m, & 2.812 \leq X_m \leq 2.84 \end{cases} \quad (31)$$

and for the WRM,

$$\frac{|V_g|}{f} = \begin{cases} 1.0007 - 0.1741X_m, & X_m \leq 1.367 \\ 1.4298 - 0.4881X_m, & 1.367 \leq X_m \leq 1.771 \\ 3.0192 - 1.3857X_m, & 1.771 \leq X_m \leq 2.0 \end{cases} \quad (32)$$

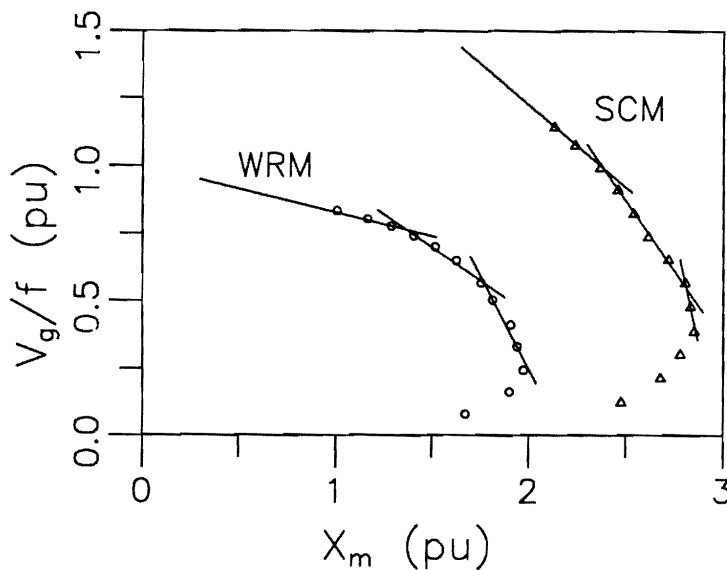


Figure 10. Characteristics of the Two Machines.

### C. Performance Equations

Once  $X_{m_i}$ 's,  $C$ , and  $f$  (or machines speeds) are known, the complete performance characteristics of all machines can be easily evaluated. Assuming  $V_t$  as the reference phasor:

$$I_{s_i} = -|V_t| \angle 0^\circ / (f Z_i) \quad (33)$$

$$|I_{r_i}| = (a_i X_{m_i} + b_i) / |Z_{r_i}| \quad (34)$$

$$P_{O_i} = \Re(V_t I_{s_i}^*) \quad (35)$$

$$P_{I_i} = v_i |I_{r_i}|^2 R_{r_i} / (f - v_i) \quad (36)$$

$$P_{L_i} = |I_{r_i}|^2 R_{r_i} + |I_{s_i}|^2 R_{s_i} \quad (37)$$

$$P_{load} = \sum_{i=1}^n P_{O_i} \quad (38)$$

where  $Z_{r_i} = R_{r_i} / (f - v_i) + j X_{r_i}$ ,  $\Re$  and  $*$  denote real part and conjugate,  $P_{I_i}$ ,  $P_{O_i}$ , and  $P_{L_i}$  are input, output and lost powers of machine "i" respectively.